Spatial Structure of Density Fluctuations and Geodesic Acoustic Mode in T-10 Tokamak.

Shelukhin D.A., Vershkov V.A., Khmara A.V.

Nuclear Fusion Institute, RRC "Kurchatov Institute", Moscow, Russian Federation

e-mail contact of main author: shelukhin@nfi.kiae.ru

Abstract. Investigation of turbulence properties could reveals the nature of anomalous transport in tokamak. This paper presents results of systematic investigations of poloidal and toroidal structure of small-scale density fluctuations as well as the properties of Geodesic Acoustic Modes (GAM) in T-10 tokamak. Improved reflectometry system allowed to made long distance toroidal correlations without parasitic cross-talk between different antennae arrays. It was found that quasi-coherent oscillations had a toroidal correlation length about 12.5 m whereas the length of stochastic low frequency fluctuations was 2.5 m. It was found some evidence of oblique propagation of the quasi-coherent oscillation at small angle (about 0.3 degree) with respect to magnetic field line. Experiments have shown that total density fluctuations amplitude is strongly non-uniform in poloidal direction. Turbulence amplitude had minimum at high magnetic field side and rise towards the low magnetic field side. The asymmetry of turbulence amplitude increased with the rise of total heating power. GAM amplitude in density fluctuations spectra was high at the top antennae positions and negligibly small at equatorial plane in accordance with theory predictions. It was reported previously that GAM exists at local electron densities lower than 2×10^{19} m^{-3} in Ohmic discharges and in the vicinity of $q = 2$ magnetic surface. Recent experiments with ECR heating have shown presence of GAM in density fluctuation spectra at high densities. Effect of the GAM on the turbulence amplitude at LFS and HFS is also discussed.

1. Introduction

The exceedance of experimental transport coefficients over neoclassical ones was found in the very first experiments in tokamak plasmas. Theory explains this phenomenon by supposing of existence additional ***turbulent*** transport mechanism driven by various instabilities. Drift instabilities are considered now as the most possible candidates for explanation of anomalous transport. Determination of the particular instabilities could give the key to suppress the transport and improve the performance of present and future machines. Such determination could be made on the base of experimental measurements of small-scale fluctuation properties.

This paper describes the results of experiments with turbulence measurements on T-10 that was made using correlation reflectometry technique [1]. The paper organized as follows. Description of T-10 tokamak and reflectometry system is given in the short introduction. The results of the toroidal correlation are presented in the section 2. It was followed by section 3 with results concerning poloidal asymmetry of turbulence amplitude. Another topic of turbulence study is the search for Zonal Flows (ZF) that now treated as the most important mechanism of turbulence amplitude saturation. Recently found peculiarities of ZF and Geodesic Acoustic Modes (GAM) are described in section 4. The summary of results is given in the end of paper.

Recent experiments continue the general line of turbulence study in T-10 tokamak [2]. T-10 is the circular cross-section machine with major radius $R = 1.5$ m and minor radius $r = 0.3$ m. It could operate with plasma currents up to 330 kA and magnetic fields up to 2.6 T. Unique feature of T-10 tokamak is 2 MW system of additional heating on second harmonic of electron cyclotron frequency (ECR) giving possibility of investigating discharges with dominant electron heating.

Turbulence was observed using correlation reflectometer [1] in several bends covering frequencies from 25 to 55 GHz. Detection of reflected signals was made by IQ detectors and

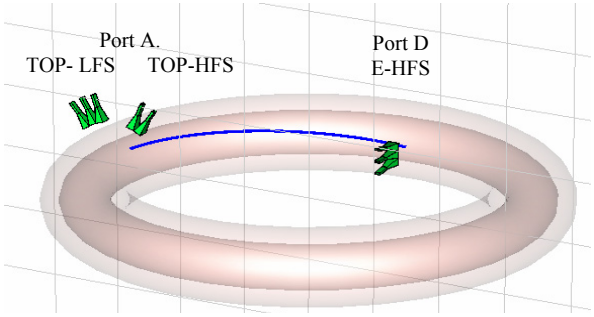

Fig.1. Reflectometer antennae arrays position in T-10 tokamak.

acquired with 1 MHz ADC, all analysis were made in complex form. Present configuration of antenna arrays at T-10 includes two antenna arrays in the top port in A cross-section, shifted at +28.5° to the vertical position to the Low Magnetic Field Side [TOP-LFS] and −26.5° to the High Magnetic Field Side [TOP-HFS], and one antenna array in the equatorial plane at HFS (EQ-HFS) in D cross-section (Fig. 1).

2. Toroidal correlation experiments

The history of long distance toroidal correlation [LDTC] investigation in T-10 has began in 2001 [1,2]. The previous T-10 reflectometry configuration with the presence of two antenna arrays in the top port, separated poloidally at 55º gives possibility to observe long distance correlation along the torus, when the magnetic field line emerging from the first antenna, passing through the sensitive spot of the second one after one turn around the tokamak. The analysis of the possible resonance conditions showed that the toroidal correlations should be observed at the magnetic surfaces with $q = 0.87$ and $q = 1.18$, provided that the turbulence does not strongly deviate from the magnetic field line. The first attempt to observe long distance correlations was done using one reflectometer, probing the plasma with the same frequency at LFS and HFS. The search of the resonant conditions by variation of the q at the reflected surface was successful. The further experimental runs, nevertheless, showed that the maxima of cross-correlations were observed not only in case of the real toroidal resonance, but also in some non-resonant conditions. The reason of arising of such parasitic maxima was direct cross-talk between LFS and HFS antennas, placed in one port. The recent installation of the antenna array at the equatorial HFS position 90° toroidally from the old antennae enables to repeat LDTC. The toroidal antennae separation guarantees the absence of the cross-talk and significantly increase the available number of resonance q values. The advantage of the new experiments was also the use of the much more informative IQ detection that allowed clearly separates different turbulence types. An example of LDTC is given on Fig. 2. On the top panel Fourier spectra of signals from two toroidal separated antennae are shown, on the middle – cross-phase and on the top – coherency between signals from two toroidal separated antennae.

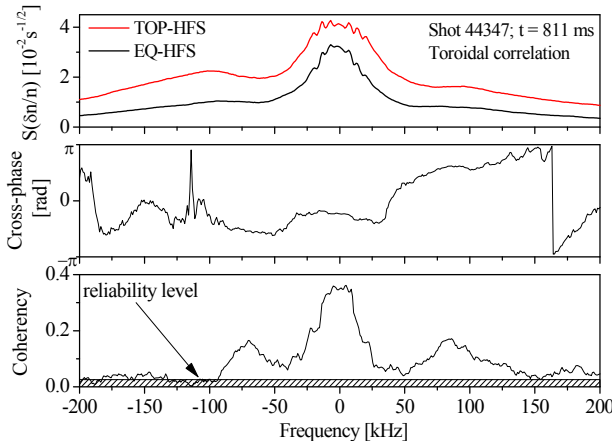

Fig.2 Top panel: spectra from two toroidally separated antennae. Middle panel: cross-phase. Bottom panel: coherency between signals from two toroidally separated antennae.

The two experimental runs were carried out at the same plasma parameters, except of the different toroidal magnetic field directions. The discharge conditions were: $I_p = 250$ кА, $B_T = 2.4$ T and density was slowly decreasing during the discharge from $\bar{n}_e = 2.5\times10^{19}$ m^{-3} to $\bar{n}_e = 2.0\times10^{19}$ m^{-3}. The decrease of the density during one discharge enabled the fine radial (and q) scan. The frequency variation of the source from discharge to discharge give possibility to cover the reflection radii from the center to the $\rho = 0.9$, thus probing the q values from 1 to 2.8. The frequency change was

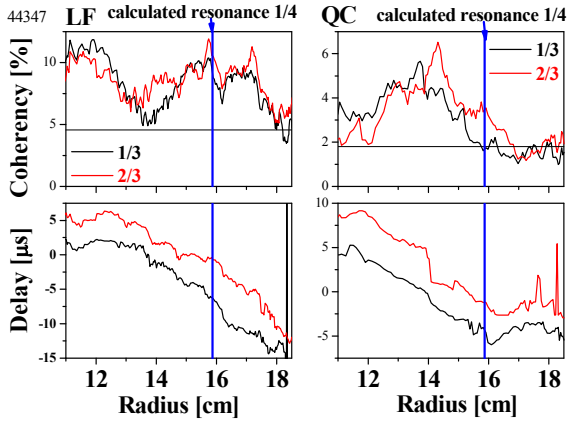

Fig. 3. Top panel: radial dependence of coherency between two toroidally separated antennae. Bottom panel: Lag of the maximum of toroidal cross-correlation function. Red and black colors correspond to different antennae pairs. Left plots present the results for LF fluctuations, right – for QC. Vertical blue lines correspond to resonance q value.

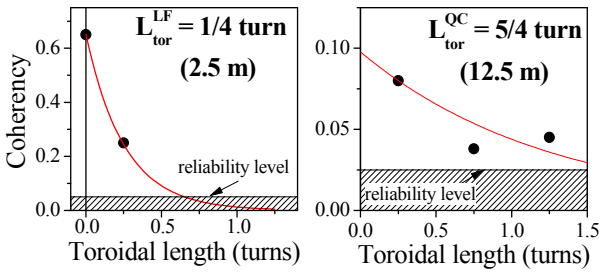

Fig. 4. Toroidal correlation functions for LF (left) and QC (right) oscillations. Points correspond to data points, red curves to approximation. Shadowed regions show reliability level

adjusted in order that the fine scans in successive shots overlapped. Such scan guaranteed the realization of the resonant conditions. The reflection radii were obtained by means of the abelization of the 16 channel interferometer data. The current profile was reconstructed from the electron temperature, taking into account neoclassical conductivity and experimentally from the $q = 2$ island position with reflectometry and $q = 1$ from sawtooth reversion radius. Both estimates were in good agreement with the calculated current profile with 1.5D code "ASTRA"

The results of the first experimental run are presented in Fig. 3. The TOP-HFS and EQ-HFS antenna arrays were used with the counterclockwise toroidal magnetic field direction. As the array EQ-HFS has three antennae, the middle one was used as the launcher and both side antennas as receivers. This gives opportunity to record simultaneously three reflected signals: one from the port A and two other from port D. Such configuration has two advantages. Firstly, it is important to note that the poloidal angles of the two antennae are slightly different and the toroidal correlations should be observed at different radii. Secondly, the two antennas in EQ-HFS give opportunity to observe the poloidal turbulence rotation in each shot. The notations of the two correlation pares in Fig. 3 are 1/3 and 2/3. As the correlations at $q_3 = 2.177$ (7/4 torus length) were lower the reliability level, thus only radial position of the resonant q value $q_1 = 1.353$ (1/4 torus length), is marked by vertical line. The resulted radial distribution of the Low Frequency oscillation (LF) and Quasi Coherent (QC) oscillations coherency are shown at the top panels in the Fig.3a,b. The time delays between the signals are presented at the lower panels of the Fig 3a,b. The black curves correspond to 1/3 and red one to 2/3 antennas. It is seen that the maxima of LF coherency coincide with the resonant q values within the accuracy +/− 1 cm, while the maximum of the QC coherency is shifted to the lower q value. The variation of the delays with the radius is very informative. Firstly the strong delay variation eliminates possibility of the presence of parasitic correlation (for parasitic signals the delays are constant). Secondly, the negative slope of the delay with radius proves that correlations occurred in the expected way. The right geometry of the correlation additionally proved by the radial shift of the 2/3 with respect to 1/3 delay.

The observed correlations values enable to estimate the correlation lengths of the LF and QC along the magnetic field line. These data can be seen in Fig. 4 a,b. The correlation lengths of the QC along the magnetic field line is longer, as it were seen at 1/4, 3/4 and 5/4 turns around the torus. The estimated correlation length is about 12.5 m. The estimations of the LF correlation length were done with the use of the poloidal correlation value at zero separation,

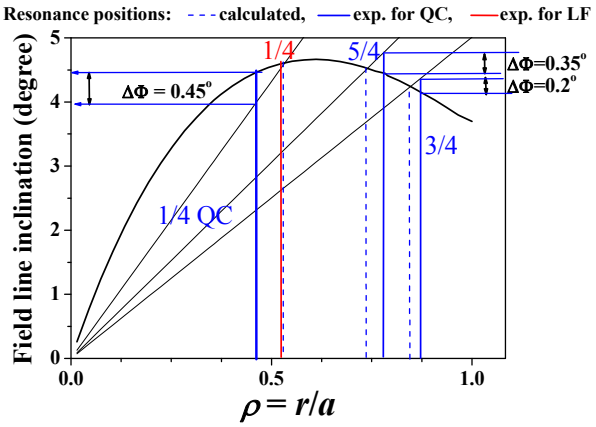

Fig. 5. Radial dependence of magnetic field line inclination. Solid red vertical line shows experimental LF resonance position, solid blue line – experimental position of QC resonances. Dashed blue vertical lines show calculated resonance q positions.

the measured value at 1/4 of the torus and reliability level at 3/4 of the torus. The value of the LF correlation length was estimated in 1/4 of the torus circumference.

The summary of the experimental data is plotted in Fig. 5. It presents the dependence of the magnetic field line angle versus minor radius. The resonant radial positions of the resonances are plotted for both experimental runs by vertical dashed blue lines. The LF 1/4 correlation is shown by solid red line, while the QC maxima by the solid blue lines. It is clearly seen that LF resonance coincides with the calculated values. In contrary, the QC maxima are slightly shifted from calculated positions. Although the shifts for 3/4 and 5/4 small and are within error bars +/− 1 cm, the shift of 1/4 is greater, then error bars. As it is seen from the Fig. 5, the maxima QC shifts correspond to the oblique propagation with the angle about 0.3° with respect to magnetic field line. This angle is expected for the drift waves. At the same time the coincidence of LF correlations with the calculated value may indicate MHD or interchange nature of the LF turbulence.

Concluding, it is possible to state that the broad band turbulence LDTC correlation was not observed even at 1/4 of the torus length. Thus this turbulence is highly stochastic with lowest values of the correlation length. The LF fluctuations have the longitudinal correlation length about 2.5 m, while QC correlation length equal to 12.5 m. The LF perturbations propagate toroidally close to the direction of the magnetic field line, while QC fluctuations propagate at the angle about 0.1 degrees with respect to the magnetic field line. The latter is typical property of the drift waves, predicted by theory, while the former is similar to the features of the MHD, or the interchange instabilities. The phenomenon of LF fluctuations should be additionally investigated in the future experiments.

3. Poloidal asymmetry of density perturbations amplitude.

Previous experiments have shown strong difference of total turbulence level in T-10 tokamak at HFS-D and LFS-A [3]. It was also reported the large difference in the kind of spectra at different poloidal angles. The next logical step was the determination of poloidal non-uniformity for different turbulence types.

Ohmic discharges with $I_p = 180$ kA, $B_T = 2.2$ T and $\bar{n}_e = 2.0\times10^{19}$ m^{-3} were chosen for analysis. The amplitude of fluctuations was estimated using 1D approach [4]. It was found that both total turbulence level and Broad Band [BB] fluctuations level has a minimum at equatorial plane at HFS and increase in 2 times towards the LFS (Fig. 6). QC oscillations show the same behaviour but the asymmetry for this turbulence type is much stronger (up to 5 times). This asymmetry could be explained in the terms of drift wave theory and be related to the toroidal curvature as a main destabilizing factor in tokamak. It was also found that LF fluctuations have a minimum amplitude and practically uniform in the poloidal direction.

Previous experiments had shown that turbulence level remains the same at HFS during ECRH heating whereas at LFS it significantly increases. This tendency was carefully analyzed in present experiments. The ratio of fluctuations amplitude at LFS to the one at HFS was used for characterization of turbulence asymmetry. The discharges with $B_T = 2.4$ T,

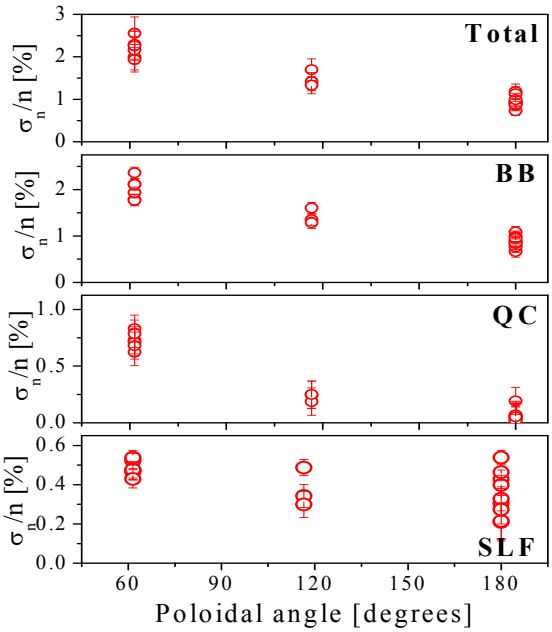

Fig. 6. Poloidal dependence of relative amplitude of density perturbations for whole turbulence spectra, BB, QC and SLF spectral components. Zero angle corresponds to equatorial plane at LFS.

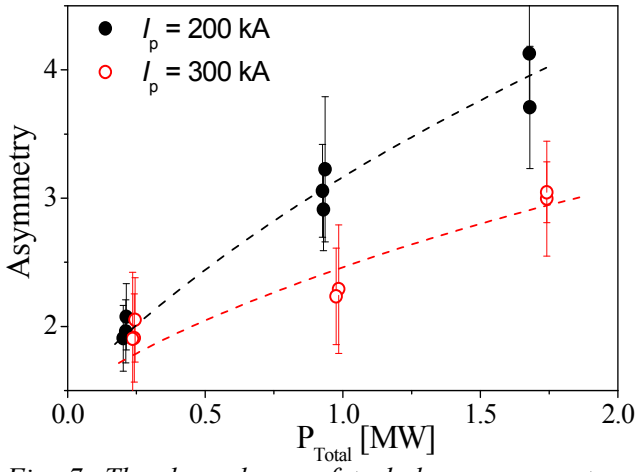

Fig. 7. The dependence of turbulence asymmetry from total heating power in ECRH discharges. Red color corresponds to discharges with plasma current 200 kA, black – to plasma current 300 kA.

$\bar{n}_e = 2.0\times10^{19}$ m^{-3} and two values of plasma current I_p = 200 kA and 300 kA were chosen for analysis (Fig. 7). On-axis ECR heating was applied to discharges with total power up to 1.7 MW. One can see clear rise of turbulence amplitude asymmetry with the rise of total power in discharge. It should be noted that asymmetry rise stronger in the case of discharges with lower plasma current, where the length of magnetic field line from LFS to HFS is longer. This fact is correlated with hypothesis that main driving force for instability exists at LFS.

4. ZF and GAM properties measurements

The search for ZF is one of the key goals of the experimental study of plasma turbulence [5]. T-10 has a long history of observation of high frequency branch of zonal flows – GAM [2,6]. Installation of antenna array at HFS allowed us to determine the poloidal structure of density perturbation in GAM oscillations in recent experiments. It was found that GAM amplitude is high at the signals reflected from the top of plasma column and negligibly small in the equatorial plane at HFS (Fig. 8). These results are perfectly correlated with TEXTOR results where it was found that GAM amplitude is close to zero in the equatorial plane at LFS [7] and theory that predict sine poloidal dependence of density perturbation by GAM [5].

Two peculiarities of GAM existence in T-10 was found in previous experiments. The first one was the existence of a maximum electron density (about 2×10^{19} m^{-3}) of GAM existence in density perturbations spectra *in Ohmic discharges*. This conclusion was justified by recent experiments with Heavy Ion Beam Probe (HIBP) diagnostic where it was found the absence of GAM in both density fluctuations and potential fluctuations spectra *in Ohmic discharges* [8]. The same phenomenon was found in ASDEX-Up experiments when GAM observed only at the periphery of plasma column [9]. Theory predicts two possible mechanisms for GAM damping. First one is Landau damping that works at low collisionalities in plateau and banana regimes and gives $\gamma \cong \omega_{GAM} \exp\left(-q^2\right)$ [10]. In T-10 experiments GAM amplitude varied with density changes at the same q value that contradict to theory predictions. Theory of GAM damping ion-ion collisions by predicts damping rate $\gamma \cong 4\nu_{ii} / 7q$ [11]. GAM amplitude in density perturbations spectra was estimated in a series

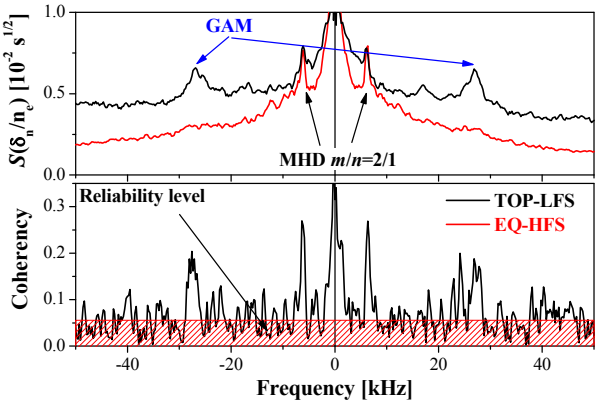

Fig. 8. Top: density perturbations spectra at top of plasma column (black curve) and in equatorial plane at HFS (red) curve. Bottom: coherency between signals from TOP-LFS and EQ-HFS antennae.

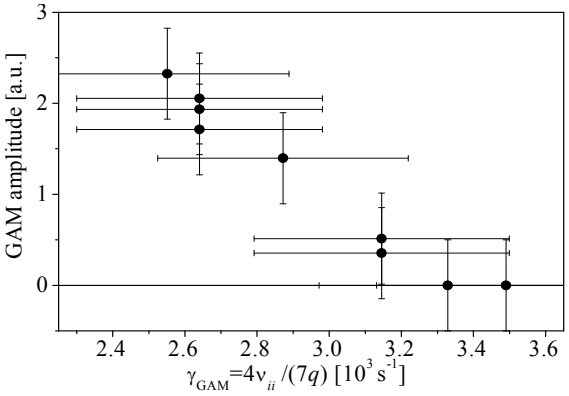

Fig. 9. Dependence of GAM amplitude in density fluctuations spectra from GAM damping rate. Discharge parameters I_p=235 kA, B_T=2.2 T, $\overline{n}_e \sim 2\times10^{19} m^{-3}$, reflection at $\rho \approx 0.75$.

of T-10 reproducible discharges with different densities (Fig. 9). Reflectometer frequency varied from discharge to discharge to keep the same radial reflection position at $\rho \approx 0.75$. One could see clear decreasing of observed GAM amplitude in with the rise of damping rate. Whereas the excitation of GAM is made by turbulence, one should expect that in extreme discharges with high level of turbulence the balance between excitation and damping moves to the higher densities. Such experiments with strong on-axis ECR heating were made in T-10 tokamak. It was found that peak in density spectra at GAM frequency observed at local electron densities up to at least 3×10^{19} m^{-3} in discharges with $B_T = 2.4$ T, $I_p = 200$ kA and 1 MW of ECRH power (Fig. 10). At the same time GAM is not observed during Ohmic phase of discharge. It should be also noted that GAM frequency during ECRH is 1.5 times higher than typical GAM frequency in Ohmic discharges. This fact is well correlated with square root dependence of GAM frequency versus electron temperature.

Another peculiarity of GAM study in T-10 tokamak was the observation of GAM only in the vicinity of $q = 2$ surface. Unfortunately in normal discharges central electron density in T-10 is higher than 2×10^{19} m^{-3} and it is impossible to found GAM oscillations. Significant improvement of wall condition after lithium gettering allowed to decrease the line averaged operation density in discharge down to 0.7×10^{19} m^{-3}. Density perturbations at GAM frequency range it was observed in the plasma core at $\rho \sim 0.3$. Simultaneous measurements from top and equatorial plane antennae show that mode had high amplitude at the top and close to zero at equatorial plane (Fig. 12). The sawteeth inversion radius ($q = 1$ position) estimated from electron cyclotron emission was found to be about $\rho \sim 0.27$. One should also found the activity in turbulence spectra at frequencies below 10 kHz. This activity could be explained by rotation of kink mode inside the $q = 1$ magnetic surface giving additional justification that reflection radius lies near $q = 1$. Experimental results shows that GAM is non-universal

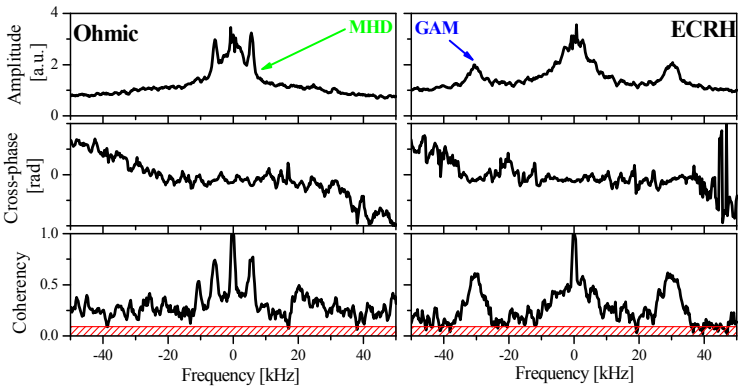

Fig. 10. Observation of GAM in high density discharges. Fourier amplitude (top), cross-phase (middle) and coherency (bottom) spectra are shown. Left panels corresponds to Ohmic phase of discharge, right – to the ECRH one.

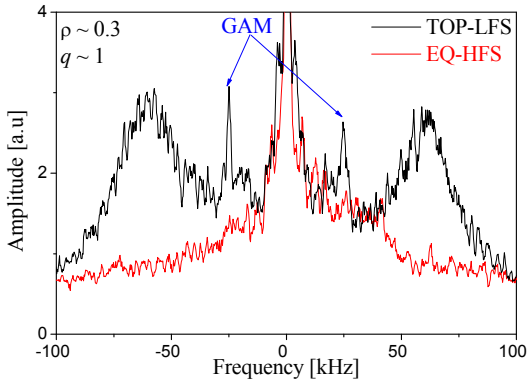

Fig. 11. Turbulence Fourier spectra at top (black) and in equatorial plane (red) in low density discharges.

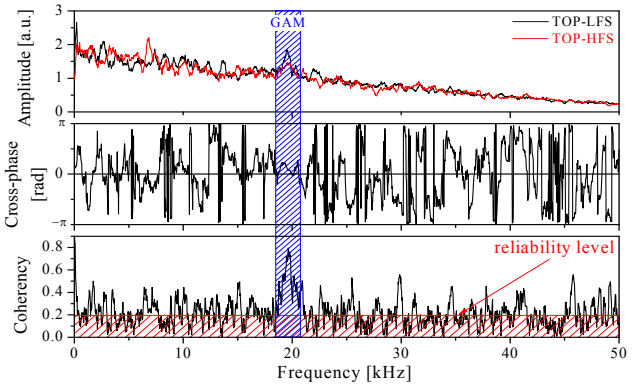

Fig. 12. Correlation analysis of perturbations of small scale density fluctuations amplitude.

phenomenon and could not explain observed quasi-stationary turbulence spectra. In contrast to GAM, Zero Mean Frequency (ZMF) branch of ZF driven by Reynold stress is often treated as a main mechanism of turbulence saturation. It should be noted that GAM is observed in most machines [12], whereas observation of ZMF branch of ZF driven by Reynold stress proclaimed only in a few experiments on CHS [13] and DIII-D [14]. T-10 measurements using HIBP and multipin Langmuir probe demonstrated that perturbations of plasma potential had the same or lesser amplitude in frequency range below 10 kHz with respect to density perturbations [6]. Poloidal velocity measurements by Doppler reflectometry in ASDEX-Up also do not show presence of ZMF zonal flows [9].

New method of data processing was applied to T-10 data to find ZMF zonal flows. One of the most important features of zonal flows is the back influence on turbulence amplitude. If ZMF zonal flows exist than turbulence amplitude on magnetic surface should varied simultaneously on whole magnetic surface and these variations could be detected using correlation technique. A set of T-10 data was analyzed in both Ohmic and ECRH discharges with local densities at reflection region from 0.8×10^{19} m^{-3} to 4.5×10^{19} m^{-3} and the reflection radii from $\rho \sim 0.4$ to $\rho \sim 0.9$. Turbulence amplitude was determined on a short time realization with moving time window for reflected signals from TOP-LFS and TOP-HFS antenna arrays. The distance between reflection points was from 12 to 27 cm that is much larger than single perturbation correlation length allowed to avoid artificial coherency due to the observation of the same perturbations in different antennae. Typical results of analysis are shown in Fig. 12 for discharge with $B_T = 2.2$ T, $I_p = 180$ kA, $\bar{n}_e = 2.0\times10^{19}$ m^{-3}, Ohmic heating, reflection at $\rho \sim 0.7$. One could see peaks in Fourier spectra at frequencies about 20 kHz that are correspond to GAM. Coherency for turbulence fluctuations at GAM frequency reaches 0.7 and has a poloidal cross-phase close to zero. This result corresponds to simultaneous modulation of density perturbations on magnetic surface by GAM in accordance with theory predictions. The same figure shows that at low frequencies coherency is of order of reliability level and no evidence of ZMF zonal flows is seen.

5. Summary

Concluding, it is possible to state that properties of QC oscillations correspond to the poloidally asymmetric perturbations of plasma density with highest amplitude at low magnetic field side. These perturbations elongated in magnetic field line direction and inclined to the magnetic field line with the angle about 0.3º. Both properties are in good agreement with theory of drift-like instabilities. BB oscillations have the same poloidal asymmetry and could also arise due to drift-like instabilities.

In the same time, LF fluctuations have rather short toroidal correlations length (~ 2.5 m) and practically uniform poloidally. Previous measurements have shown that LF had the largest poloidal and radial correlation length up to 4-8 cm [2]. Amplitude and specter of this turbulence type is seems to be insensible to the discharge conditions and exists even inside the transport barriers. The properties of this turbulence type could not be described in terms of MHD or drift instabilities so the origin of these LF fluctuations is still under consideration.

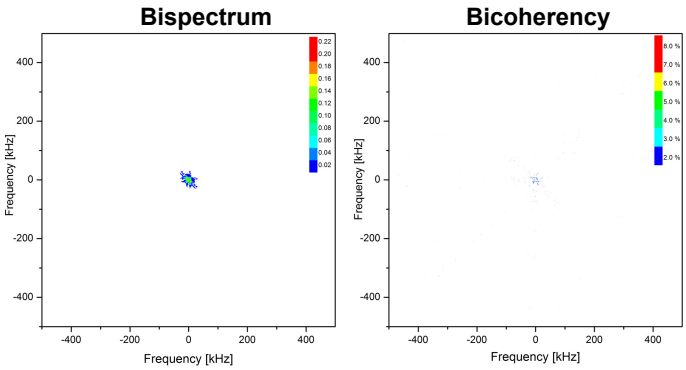

Fig 13. Bispectrum and bicoherency analysis of reflectometer signals. White color corresponds to the Gaussian noise level with dispersion equal to dispersion of analyzed signals.

It was justified the poloidal structure of density perturbations by GAM. Recent experiments demonstrated that GAM exists in more wide range of discharge parameters. Particularly GAM exists in ECR heated discharges with high densities; GAM was also be found in plasma core in the vicinity of $q = 1$ surface in discharges with low densities.

No evidence of zero mean frequency zonal flows was found in T-10 experiments. The absence of correlations in ZMF zonal flows frequency region could have two possible explanations. The first one is that ZMF zonal flows are not perturb the density fluctuations amplitude; the second one is that ZMF zonal flows is not exist in T-10 tokamak in investigated discharge parameters range. In both cases it should be some another mechanism of quasi-stationary turbulence spectra formation. Bispectra and bicoherency analysis have shown that density fluctuations are independent and have Gaussian statistic (Fig. 13) and no evidence of direct cascades is seen. Thus the question of the mechanism of non-linear turbulence amplitude saturations remains uncertain.

This work is supported by Rosatom and Grants RFBR 05-02-17016, NSh-2264.2006.2, INTAS 100008-8046 and NWO-RFBR 047.016.015.

[1] Vershkov V.A., *et al*, Rev. Sci. Instrum., 1999. **70** (3), 1700
[2] Vershkov V.A., *et al*, Nucl. Fusion, 2005, **45** (10), S203
[3] D.A. Shelukhin, *et al*, Proc. of 33th EPS Conference on Contr. Fus. and Plasma Phys., Roma, Italy, 2006, **30F**, P - 4.081.
[4] D.A. Shelukhin, *et al*, Plasma Physics Reports, 2006, **32** (9), 707
[5] P.H. Diamond *et al*, Plasma Phys. Contr. Fusion, 2005, **47** (5), R35
[6] A.V. Melnikov, *et al*, Plasma Phys. Contr. Fusion 2006, **48**, S87
[7] A. Krämer-Flecken *et al*, Phys. Rev. Lett., 2006, **97**, 045006
[8] A.V. Melnikov *et al*, this conference
[9] G.D. Conway, *et al*, Plasma Phys Contr. Fusion, 2008, **50**, 055009 (pp18)
[10] V. B. Lebedev, *et al*, Phys. Plasmas, 1996, **3** (8), 3024
[11] S. V. Novakovskii, *et al*, Phys. Plasmas, 1997, Phys. Plasmas **4** (12), 4272
[12] A. Fujisawa, *et al*, Nuclear Fusion, 2007, **47**, S718
[13] A. Fujisawa, *et al*, Plasma Phys. Control. Fusion, 2006, **48,** A365
[14] G.R. McKee, *et al*, Proc. of 21th IAEA Fus. Ener. Conf., Chengdu, China, 2006, EX/2-3